

---

01 Jan 2013

## Picturing Electron Capture to the Continuum in the Transfer Ionization of Intermediate-Energy He<sup>2+</sup> Collisions with Argon

Ruitian Zhang

Xinwen Ma

Shaofeng Zhang

Xiaolong Zhu

*et. al.* For a complete list of authors, see [https://scholarsmine.mst.edu/phys\\_facwork/1511](https://scholarsmine.mst.edu/phys_facwork/1511)

Follow this and additional works at: [https://scholarsmine.mst.edu/phys\\_facwork](https://scholarsmine.mst.edu/phys_facwork)

 Part of the [Physics Commons](#)

---

### Recommended Citation

R. Zhang and X. Ma and S. Zhang and X. Zhu and S. Akula and D. H. Madison and B. Li and D. Qian and W. Feng and D. Guo and H. Liu and S. Yan and P. Zhang and S. Xu and X. Chen, "Picturing Electron Capture to the Continuum in the Transfer Ionization of Intermediate-Energy He<sup>2+</sup> Collisions with Argon," *Physical Review A - Atomic, Molecular, and Optical Physics*, vol. 87, no. 1, pp. 012701-1-012701-5, American Physical Society (APS), Jan 2013.

The definitive version is available at <https://doi.org/10.1103/PhysRevA.87.012701>

This Article - Journal is brought to you for free and open access by Scholars' Mine. It has been accepted for inclusion in Physics Faculty Research & Creative Works by an authorized administrator of Scholars' Mine. This work is protected by U. S. Copyright Law. Unauthorized use including reproduction for redistribution requires the permission of the copyright holder. For more information, please contact [scholarsmine@mst.edu](mailto:scholarsmine@mst.edu).

## Picturing electron capture to the continuum in the transfer ionization of intermediate-energy $\text{He}^{2+}$ collisions with argon

R. T. Zhang,<sup>1,2,3</sup> X. Ma,<sup>1,\*</sup> S. F. Zhang,<sup>1</sup> X. L. Zhu,<sup>1</sup> Susmitha Akula,<sup>4</sup> D. H. Madison,<sup>4</sup> B. Li,<sup>1</sup> D. B. Qian,<sup>1</sup> W. T. Feng,<sup>1</sup> D. L. Guo,<sup>1,3</sup> H. P. Liu,<sup>1</sup> S. C. Yan,<sup>1</sup> P. J. Zhang,<sup>1,3</sup> S. Xu,<sup>1</sup> and X. M. Chen<sup>2</sup>

<sup>1</sup>*Institute of Modern Physics, Chinese Academy of Sciences, Lanzhou 730000, China*

<sup>2</sup>*School of Nuclear Science and Technology, Lanzhou University, Lanzhou 730000, China*

<sup>3</sup>*University of Chinese Academy of Sciences, Beijing 10004, China*

<sup>4</sup>*University of Missouri—Rolla, 1870 Miner Circle, Rolla, Missouri 65409, USA*

(Received 22 November 2012; published 2 January 2013)

Electron emission occurring in transfer ionization for  $\text{He}^{2+}$  collisions with argon has been investigated using cold target recoil ion momentum spectroscopy. The double differential cross sections for electron capture to the continuum of the projectile (cusp-shaped electrons) are presented for collision energies from 17.5 to 75 keV/u. For an energy of 30 keV/u, we find a maximum in the experimental ratio of the cusp-shaped electron yield to the total electron yield. This result is explained in terms of the velocity matching between the projectile ion and the electron initially bound to the target. One of the important issues for double electron transitions is the role of electron-electron correlation. If this correlation is weak, then the transfer-ionization process can be viewed as two separate sequential processes. If this correlation is strong, then the transfer-ionization process would happen simultaneously and not sequentially. Our experimental and theoretical results indicate that correlation is weak and that the first step is target ionization followed by charge capture.

DOI: [10.1103/PhysRevA.87.012701](https://doi.org/10.1103/PhysRevA.87.012701)

PACS number(s): 34.50.-s, 34.70.+e

### I. INTRODUCTION

Studies of doubly differential cross sections (DDCS) for electron ejection provide valuable information about the physical mechanisms controlling the ionization processes, such as single ionization (SI) and transfer ionization (TI). One of the prominent features, first observed by Crooks and Rudd for SI [1], is a characteristic cusp-shaped peak in the energy spectrum for forward emitted electrons. Crooks and Rudd called this feature electron capture to the continuum (ECC). Most of the early experiments and quantum theories of the cusp shape focused on single-ionization processes [1–8] in which the cusp shape was considered as a smooth transition linking the electron captured to the bound states of the projectile and the continuum states of the target [2]. Due to the experimental difficulties associated with measuring DDCS for two-electron transitions, the emission of cusp-shaped electrons has received little attention for transfer ionization.

On the other hand, the important collision mechanisms for energetic ion-atom collisions have been of continuing interest since the early work of Brinkman and Kramers [9]. For example, Sidky and Simonsen [10] have proposed that the transfer amplitude increases if the velocity of the valence target electron matches the projectile velocity. Schippers *et al.* [11] stated that the total capture probability should be proportional to an overlap of the initial and the final states shifted by the projectile's velocity in momentum space. More recently, with the kinematically complete measurement techniques, it has been confirmed that increasing the projectile velocity (larger than matching velocities) leads to a preference of capture to the ground state of the projectile [12,13]. Comparing with the charge exchange processes, Madison and Manson [14] concluded that the ionization cross sections for a subshell reach

a maximum when the incident projectile ion travels at a speed near the electron's orbital velocity. Likewise, Ning *et al.* [15] studied the dependence of the cusp-shaped electron yield on the projectile velocity in single ionization using the continuum distorted wave–eikonal initial state (CDW-EIS) approach. In general it was found that the cusp electrons can be attributed to a “velocity-matching” mechanism, namely, the probability increases as the projectile velocity matches the bound electron's most probable orbital velocity and then the probability falls off as the projectile velocity goes beyond the matching velocity. Therefore, the phenomenon of velocity matching is a general feature for charge transfer and ionization in ion-atom collisions. Here, we are studying it for the case of transfer ionization.

We are studying the following collision:



For this process, one electron is transferred (i.e., captured) and one electron is ionized so we will label it as TIII. It is only very recently that experimental technology has advanced to the point where detailed studies of a process in which two electrons change states can be studied. One of the first important questions concerning two-electron processes is whether the two transitions are uncorrelated and proceed in sequential steps or whether they are highly correlated and essentially happen simultaneously. If they are uncorrelated, then the electron-electron interaction does not play an important role and the question turns to which process happens first—ionization or capture. We can get a good idea about the importance of correlation by comparing TI results with SI results. For example, if correlation is not important and ionization occurs first, the TIII results should be similar to single ionization of a neutral target by  $\text{He}^{2+}$  [16]. On the other hand, if correlation is not important and capture occurs first, then the TIII results should be similar to single ionization of  $\text{Ar}^+$  by  $\text{He}^+$ . If, on the

\*x.ma@impcas.ac.cn

other hand, TIII results are very different from either  $\text{He}^{2+}$  ionization of Ar or  $\text{He}^+$  ionization of  $\text{Ar}^+$ , then correlation is likely to be very important and change the shape of the cross sections.

In this paper, we will present DDCCS results as a function of ejected-electron energy for small emission angles and demonstrate that, similar to ECC for single ionization, we find a sharp peak when the projectile velocity matches the ejected-electron velocity. We will then compare experimental and theoretical total cross sections (TCSs) integrated over ejected-electron energies and angles. This comparison reveals a strong similarity between TIII and  $\text{He}^{2+}$  ionization of Ar which suggests that correlation is weak and single ionization occurs first.

## II. EXPERIMENTAL SETUP

We have performed experiments for transfer ionization in 17.5–75 keV/u  $\text{He}^{2+}$ -Ar collisions using the cold target recoil ion momentum spectroscopy (COLTRIMS) apparatus at the 320-kV platform for multidiscipline research with highly charged ions at the Institute of Modern Physics, Lanzhou. The experimental technique of COLTRIMS has been described in detail in Refs. [17,18]. Briefly, the  $\text{He}^{2+}$  ions produced in the electron cyclotron resonance (ECR) ion source are first charge selected by an analyzing magnet, and then accelerated to the desired energy when they leave the high voltage platform. The ion beam is collimated by two sets of four-jaw adjustable slits before entering the collision chamber. The vacuum is better than  $10^{-9}$  mbar in the beam line. In order to clean the contamination due to the interaction between the primary beam and residual gas in the path before the target chamber, several sets of electrostatic deflectors are installed in the front of the collision region. The ion beam ( $z$  direction) intersects with a supersonic gas jet ( $y$  direction) at  $90^\circ$  in the center of the time-of-flight (TOF) spectrometer. A weak electrostatic field of 1.8 V/cm perpendicular to the ion beam and the gas jet ( $x$  direction) is used to extract the recoil ions and the electrons from the collision area in opposite directions. A homogeneous magnetic field parallel to the electric field causes the electrons to move on spiral trajectories from the reaction volume to the detector. The positions of the recoil ions and the electrons are recorded by two two-dimensional position sensitive detectors placed on the opposite ends of the TOF spectrometer (the  $yz$  plane). The length ratio of the accelerating region and the drifting region of the TOF spectrometer is 1 to 2 which meets the time focusing condition in order to reduce momentum broadening caused by the target gas spread [19]. The projectiles with different charge states are analyzed by an electrostatic deflector downstream from the collision center, directed to a position sensitive detector. From the experimentally determined flight time and the charge state, the initial momentum of the recoil ion parallel to the field direction can be obtained. Combined with the position information on the recoil detector, the other two components perpendicular to the field direction can also be calculated. Similarly, electron momentum vectors can also be reconstructed. The electron energy resolution depends on the kinematic energy. The estimated energy resolution is better than 0.3 eV for electron energy less than 1 eV, and it is

about 1 eV for electron energy equal to 10 eV, for example. The factors which influence the momentum resolution of the recoil ions and the electrons for the spectrometer have been investigated in detail [20].

In our experiment, the triple coincidence between recoil ions, scattered projectile ions, and outgoing electrons was performed. From the two-dimensional spectrum of recoil ions' flight time versus the scattered ion position, at least seven transfer-ionization reaction channels are identified [18]. Atomic units are used throughout the paper, except when otherwise stated.

## III. RESULTS AND DISCUSSION

The experimental results for double differential cross sections (DDCCS) with respect to the electron energy and the electron emission angle were measured. Absolute cross sections for the electron emission were obtained by integrating the measured differential cross sections and normalizing to the cross sections reported by DuBois [21]. In the present paper, only statistical errors are presented. This section is organized as follows. Section I gives an overview of the cusp-shaped (EEC) spectra, for projectile energies of 17.5, 25, 30, 50, and 75 keV/u. A discussion of the velocity matching mechanism for cusp-shaped electron emission in TIII processes are presented in Sec. II.

### A. Double differential cross sections for cusp-shaped electron emission

The DDCCS of emitted electrons is traditionally obtained by scanning the energy and angles of the electrons ejected in the energetic ion-atom collisions. Our measured DDCCS with respect to the energy and angle of the ejected electron is shown in Fig. 1 for projectile energies of 17.5, 25, 30, 50, and 75 keV/u, respectively. Here, we primarily focus on the DDCCS for cusp-shaped electron emission which is known to occur for small projectile scattering angles. Consequently, we restrict the electron emission angles to  $0^\circ$ – $3^\circ$ . The vertical lines on the plot show the energy corresponding to velocity matching between the projectile and the ejected electron.

As shown in Fig. 1, cross sections for the cusp-shaped electrons gradually decrease as the projectile energy is increased. For relatively low projectile energies, cusp-shaped peaks are slightly shifted to lower energies than the positions expected for velocity matching with the ejected electron (short vertical line). The cusp peaks also show a strong asymmetry. These two features have been explained in terms of the postcollision attraction between the target ion and the ionized electron after the ECC [22]. It is a general effect that is enhanced for the lower projectile energies. The other feature of cusp-shaped peak is that it becomes broader with increasing projectile energy. It is reported that the full width at half maximum (FWHM) increases linearly with the projectile velocity [23]. Considering this effect and the spectrometer resolution, the estimated FWHM for the cusp electrons are 3.9, 4.7, 5.3, 7.2, and 9.0 eV for projectile energies of 17.5, 25, 30, 50, and 75 keV/u, respectively. Clearly, the FWHM is smaller than the measured value shown in Fig. 1. The reason will be studied in the future using more data sets and different collision systems.

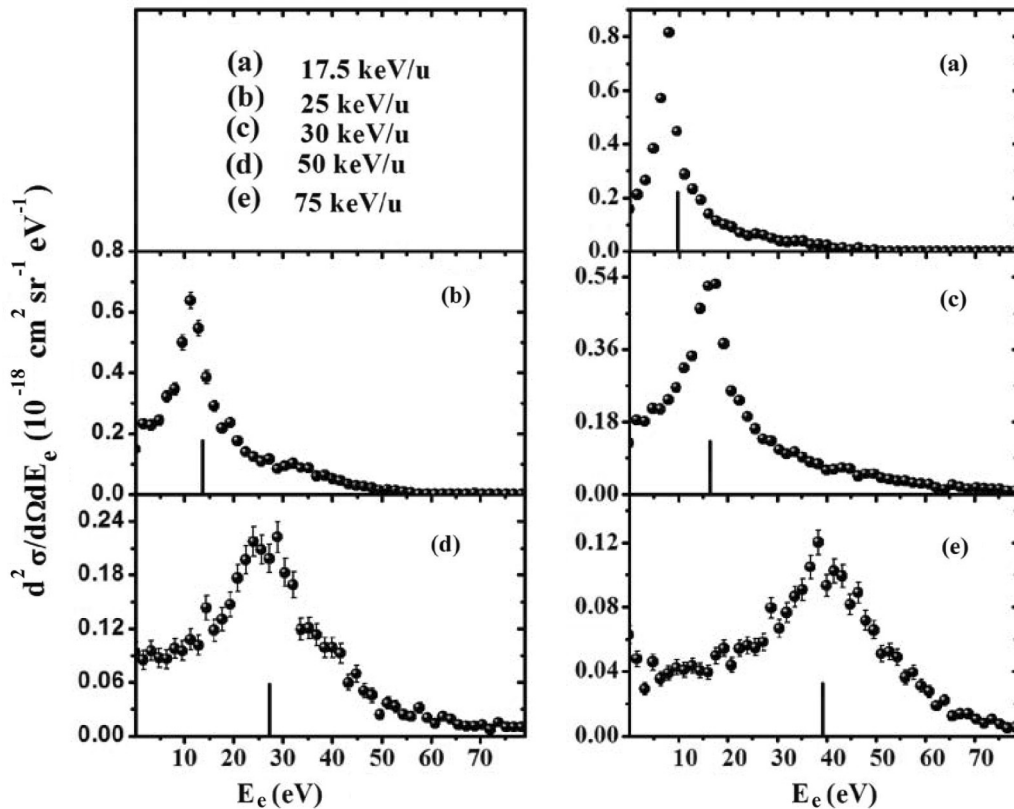


FIG. 1. Double differential cross sections as a function of the ejected-electron energy for electrons emitted within  $0^\circ$ – $3^\circ$ . The projectile energies are 17.5, 25, 30, 50, and 75 keV/u, respectively. The short vertical lines represent the position of velocity match between the projectile and the ejected electron.

### B. Velocity matching mechanism for cusp-shaped electron emission

To our knowledge, the only theoretical work for transfer-ionization is limited to collisions with helium [24–27]. For heavier targets, there has been considerable theoretical work for single ionization [14] without transfer and we can use these results to determine the important physical mechanisms qualitatively. Based on the systematic experimental studies of transfer ionization for  $\text{He}^{2+}$  collision with argon by Viktor *et al.* [28], it was concluded that the electron emission pattern is independent of the final state of the bound electron, i.e., the cusp electron production for transfer ionization in  $\text{He}^{2+}$  collision with argon could be separated into two independent processes.

In Fig. 2, we show the dependence of the experimental ratio of cusp-shaped electrons to the total intensity of ejected electrons [i.e., the total cross section (TCS)] for projectile energies of 17.5, 25, 30, 50, and 75 keV/u, respectively. The corresponding cusp-shaped contributions are evaluated to be 0.78%, 0.9%, 0.96%, 0.6%, and 0.35% of the total electron yield, respectively. It is clear, however, that the TCS ratios are very sensitive to the projectile energies and that there is a maximum in the vicinity of 30 keV/u. The maximum at 30 keV/u in the TCS corresponds to a projectile velocity  $v_p$  of (1.1 a.u.) which matches the initial value for the bound  $3p$  orbital electron velocity of Ar. This observation was predicted by Sidky and Simonsen [10], based on the early work of Brinkman

and Kramers [9], “the total possibility of electron capture to the continuum should be proportional to an overlap of the initial and final states in the momentum space, when the orbital mean velocity of the target’s electron matches the speed of the passing ion.” That is, the relative yield of cusp-shaped electrons reaches a maximum for velocity matching conditions.

As mentioned above, the experimental results of Viktor *et al.* [28] suggest that transfer ionization proceeds as two independent processes. If this is the case, then the next question concerns the order of the processes. Bernardi *et al.* [29] have proposed that the first step is ionization, followed by

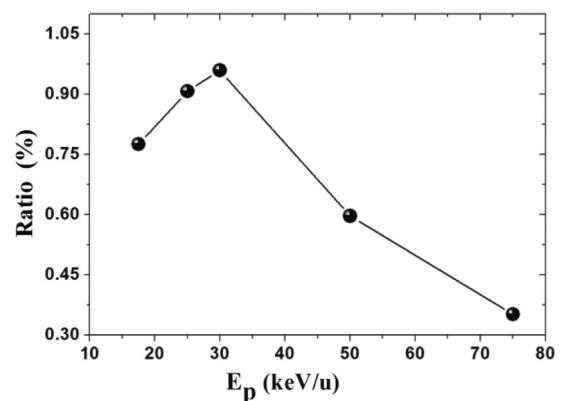


FIG. 2. The ratio of cusp-shaped electrons to the total electrons ejected in transfer ionization. The line is a guide for the eyes.

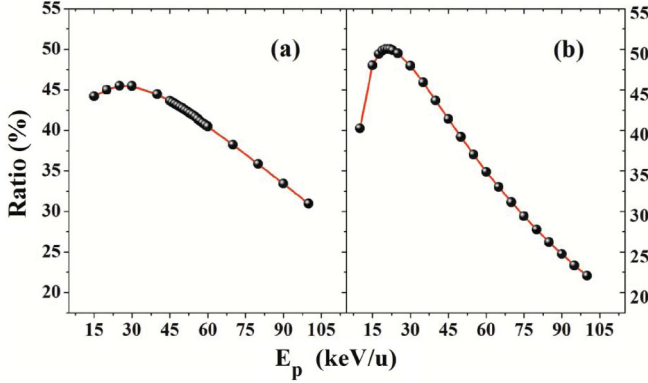


FIG. 3. (Color online) Theoretical PWBA TCS ratios of cusp-shaped electrons to the total electrons ejected in the single ionization of Ar and  $\text{Ar}^+$ . (a) Theoretical results for  $\text{He}^+$  ionizing  $\text{Ar}^+$ ; (b) theoretical results for  $\text{He}^{2+}$  ionizing Ar. Lines are a guide for the eyes.

capture. To test these two assumptions, we have calculated theoretical single-ionization results using the plane wave Born approximation (PWBA) approach of Madison and Manson [14]. In this approach, the projectile is treated as a plane wave both initially and finally, and the ejected electron is treated as a distorted wave in the field of the residual ion. The EEC contribution is included using the Salin approximation [30]. Figure 3 presents the fraction of the EEC contribution to the TCS as a function of the incident projectile energy for  $\text{He}^+$  ionizing  $\text{Ar}^+$  [Fig 3(a)] and  $\text{He}^{2+}$  ionizing Ar [Fig 3(b)]. As reported by DuBois [21], the cross sections for total electron emission do not show a strong energy dependence for the present range of projectile energies. If the capture of one electron is largely independent of the ejection of another electron, electron ejection in T1I1 should resemble that of single ionization (SI). Similarly, cusp electron (ECC) contributions to T1I1 processes should also have the same shape as SI. Comparing our experimental data in Fig. 2 with the theoretical calculations in Fig. 3, it is seen that both theoretical calculations for SI have a similar shape to T1I1 which supports the two-independent-step model. It is also seen that the cross section for  $\text{He}^{2+}$  ionizing Ar [Fig 3(b)] gives the better overall shape agreement with experiment, particularly for the higher energies. This observation, coupled with the fact that the magnitude of the SI cross section for  $\text{He}^{2+}$  ionizing Ar is about a factor of 16 times larger than the SI cross section for  $\text{He}^+$  ionizing  $\text{Ar}^+$  provides additional evidence that the cusp electrons dominantly originate from first ionization and then capture in the present reaction channel. However, there is a factor of about 50 difference in magnitude between ratios in T1I1 and SI resulting from the fact that the cross sections for two-electron processes are well known to be one to two orders of magnitude smaller than corresponding one-electron processes.

An additional piece of evidence comes from the longitudinal momentum of the recoil ion which is given by Ref. [17]

$$P_{R,\parallel} = \frac{-Q}{v_p} - v_p + \frac{(v_e - v_p)^2}{2v_p}. \quad (2)$$

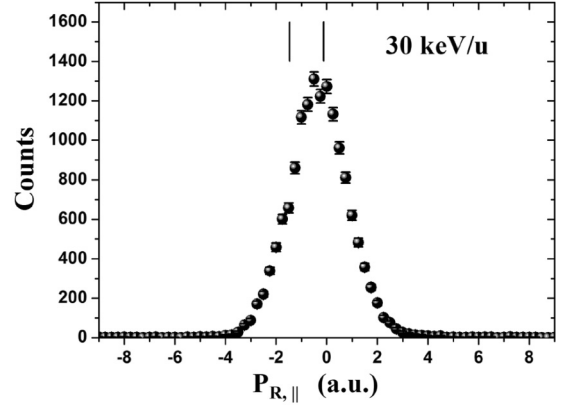


FIG. 4. Longitudinal momentum distribution of recoil ions associated with the cusp-shaped processes (ECC) for T1I1 in 30 keV/u  $\text{He}^{2+}$  collisions with argon. The left and the right vertical lines correspond to electrons captured to the ground state and first excited state of the projectile without target excitation, respectively.

Here  $P_{R,\parallel}$  is the longitudinal momentum of recoil ion,  $Q$  denotes the change in internal energies of the projectile and the target,  $v_p$  is the projectile velocity, and  $v_e$  is the ejected-electron velocity. For the case of ECC, the third item in Eq. (2) would be neglected. If ionization occurs first, the  $3p$  electron of the  $\text{Ar}^+$  ion would prefer to capture into the first excited state of  $\text{He}^+$  rather than capture to the ground state due to the much smaller  $Q$  value. In Fig. 4 we present the measured longitudinal momentum for the case of 30 keV/u  $\text{He}^{2+}$  collision with argon. Also shown in Fig. 4 are two vertical lines representing the longitudinal momentum calculated from Eq. (2). The left vertical line corresponds to the longitudinal momentum for electrons captured into the ground state of the projectile and the right vertical line corresponds to the longitudinal momentum for electrons captured into the first excited state. It is seen that the measured longitudinal momentum distribution peaks at the momentum corresponding to capture to the first excited state. Consequently, this is further evidence supporting ionization as the first step. However, due to the poor momentum resolution of the heavy target, the left vertical line overlaps a significant part of the distribution which might suggest that, while ionization first dominates, there are nevertheless a nonignorable number of cases where capture is the first step. We should also note that there are other possible processes such as simultaneous target excitation [20,31] that should be considered.

#### IV. SUMMARY

Using the COLTRIMS technique, a kinematically complete experiment has been performed to investigate the cusp-shaped electron emission in transfer ionization for  $\text{He}^{2+}$ -argon collisions at impact energies of 17.5, 25, 30, 50, and 75 keV/u. For doubly differential cross sections (differential in the ejected-electron energy and its emission angle), the cross sections for small ejection angles peaked when the ejected-electron velocity was close to the projectile velocity. We also integrated the DDCCS over electron-ejection angles and energies to get the total cross section as a function of incident projectile energies. For the total cross sections, we determined

the experimental ratio of the cusp-shaped electron yield to the total electron yield as a function of collision energy. We found a strong energy dependence for this ratio which reached its maximum when the projectile velocity matched that of the 3p electron.

Previous studies have suggested that the process of transfer ionization can be regarded as two independent events and that the first step is single ionization followed by single capture. We investigated this hypothesis by comparing theoretical and experimental total cross sections as well as the longitudinal momentum distribution of recoil ions associated with the cusp-shaped processes. The total cross section comparison showed that the SI total cross sections are very similar to the TIII cross sections which would indicate two independent processes. Further, the shape of the SI cross section for He<sup>2+</sup> ionization of argon was closer to the TIII cross sections and the magnitude of the cross section for He<sup>2+</sup> ionization

of argon was more than a factor of 10 times larger than the SI cross section for He<sup>+</sup> ionizing Ar<sup>+</sup>. These results suggest that the first step is ionization. Finally the experimental and theoretical results for the longitudinal momentum distribution of recoil ions also indicated that ionization was the first step. However, both of these comparisons also indicated that, although ionization first is the dominant process, capture first also makes a non-negligible contribution.

#### ACKNOWLEDGMENTS

This work was supported by the Major State Basic Research Development Program of China (973 Program, Grant No. 2010CB832902) and by the National Natural Science Foundation of China under Grants No. 10979007 and No. 10974207. S.A. and D.H.M. gratefully acknowledge support of the US National Science Foundation under Grant No. PHY-1068237.

- 
- [1] G. B. Crooks and M. E. Rudd, *Phys. Rev. Lett.* **25**, 1599 (1970).  
 [2] M. E. Rudd and J. Macek, *Case Stud. At. Phys.* **3**, 125 (1972).  
 [3] M. W. Lucas and K. G. Harrison, *J. Phys. B: At. Mol. Phys.* **5**, L20 (1972).  
 [4] W. Oswald, R. Schramm, and H. D. Betz, *Phys. Rev. Lett.* **62**, 1114 (1989).  
 [5] R. G. Pregliasco, C. R. Garibotti, and R. O. Barrachina, *J. Phys. B: At. Mol. Opt. Phys.* **27**, 1151 (1994).  
 [6] D. H. Lee, P. Richard, T. J. M. Zouros, J. M. Sanders, J. L. Shinpaugh, and H. Hidmi, *Phys. Rev. A* **41**, 4816 (1990).  
 [7] Y. D. Wang, V. D. Rodríguez, C. D. Lin, C. L. Cocke, S. Kravis, M. Abdallah, and R. Dörner, *Phys. Rev. A* **53**, 3278 (1996).  
 [8] R. E. Olson and A. Salop, *Phys. Rev. A* **16**, 531 (1977).  
 [9] H. C. Brinkman and H. A. Kramers, *Proc. Acad. Sci. Amsterdam* **33**, 973 (1930).  
 [10] E. Y. Sidky and Hans-Jorgen T. Simonsen, *Phys. Rev. A* **54**, 1417 (1996).  
 [11] S. Schippers, A. R. Schlatmann, and R. Morgenstern, *Phys. Lett. A* **181**, 80 (1993).  
 [12] T. Kambara, M. Kimura, Y. Awaya, T. M. Kojima, V. Mergel, Y. Nakai, and H. Schmidt-Böcking, *J. Phys. B: At. Mol. Phys.* **31**, L909 (1998).  
 [13] V. Mergel, R. Dörner, J. Ullrich, O. Jagutzki, S. Lencinas, S. Nüttgens, L. Spielberger, M. Unverzagt, C. L. Cocke, R. E. Olson, M. Schulz, U. Buck, E. Zanger, W. Theisinger, M. Isser, S. Geis, and H. Schmidt-Böcking, *Phys. Rev. Lett.* **74**, 2200 (1995).  
 [14] D. H. Madison and S. T. Manson, *Phys. Rev. A* **20**, 825 (1979); M. E. Rudd, Y. K. Kim, D. H. Madison, and J. W. Gallagher, *Rev. Mod. Phys.* **57**, 965 (1985); M. E. Rudd, Y. K. Kim, D. H. Madison, and T. J. Gay, *ibid.* **64**, 441 (1992).  
 [15] Y. Ning, B. He, C. L. Liu, J. Yan, and J. G. Wang, *Phys. Rev. A* **72**, 022702 (2005).  
 [16] M. Schulz, X. Wang, M. Gundmundsson, K. Schneider, A. Kelkar, A. B. Voitkiv, B. Najjari, M. Schöffler, L. Ph. H. Schmidt, R. Dörner, J. Ullrich, R. Moshhammer, and D. Fischer, *Phys. Rev. Lett.* **108**, 043202 (2012).  
 [17] J. Ullrich, R. Moshhammer, A. Dorn, R. Dörner, L. P. H. Schmidt, and H. Schmidt-Böcking, *Rep. Prog. Phys.* **66**, 1463 (2003).  
 [18] X. Ma, R. T. Zhang, S. F. Zhang, X. L. Zhu, W. T. Feng, D. L. Guo, B. Li, H. P. Liu, C. Y. Li, J. G. Wang, S. C. Yan, P. J. Zhang, and Q. Wang, *Phys. Rev. A* **83**, 052707 (2011).  
 [19] W. C. Wiley and I. H. McLaren, *Rev. Sci. Instrum.* **26**, 1150 (1955).  
 [20] D. L. Guo, X. Ma, W. T. Feng, S. F. Zhang, and X. L. Zhu, *Acta Phys. Sin.* **60**, 11 (2011).  
 [21] R. D. DuBois, *Phys. Rev. A* **36**, 2585 (1987).  
 [22] M. B. Shah, C. McGrath, C. Illescas, B. Pons, A. Riera, H. Luna, D. S. F. Crothers, S. F. C. O'Rourke, and H. B. Gilbody, *Phys. Rev. A* **67**, 010704(R) (2003).  
 [23] W. Meckbach, B. Nemirovsky, and C. R. Garibotti, *Phys. Rev. A* **24**, 1793 (1981).  
 [24] M. S. Schöffler, A. L. Godunov, and H. Schmidt-Böcking, *J. Phys. B* **38**, L123 (2005).  
 [25] A. L. Godunov, C. T. Whelan, H. R. J. Walters, V. S. Shipakov, M. Schöffler, V. Mergel, R. Dörner, O. Jagutzki, L. Ph. H. Schmidt, J. Titze, and H. Schmidt-Böcking, *Phys. Rev. A* **71**, 052712 (2005).  
 [26] H.-K. Kim, M. S. Schöffler, S. Houamer, O. Chuluunbaatar, J. N. Titze, L. Ph. H. Schmidt, T. Jahnke, H. Schmidt-Böcking, A. Galstyan, Yu. V. Popov, and R. Dörner, *Phys. Rev. A* **85**, 022707 (2012).  
 [27] M. Zapukhlyak and T. Kirchner, *Phys. Rev. A* **80**, 062705 (2009).  
 [28] L. Viktor, L. Sarkadi, A. Báder, D. Berényi, J. A. Tanis, M. Kuzel, K. O. Groeneveld, and P. A. Závodszky, *Nucl. Instrum. Methods Phys. Res., Sect. B* **124**, 342 (1997).  
 [29] G. Bernardi, P. Focke, and W. Meckbach, *Phys. Rev. A* **55**, R3983 (1997).  
 [30] A. Salin, *J. Phys. B: At. Mol. Phys.* **5**, 979 (1972).  
 [31] U. Chowdhury, A. L. Harris, and D. H. Madison, *J. Phys. B: At. Mol. Phys.* **45**, 175204 (2012).